Synthesis and Structure of Redox-Active Heterotetranuclear Molecular Polygons by Self-Assembly of Two Ferrocene-Bridged Bis(pyridines) with Two Transition Metals[‡]

Ekkehard Lindner,*[a] Ruifa Zong,[a] Klaus Eichele,[a] Ulrike Weisser,[a] and Markus Ströbele[a]

Keywords: Self-assembly / Nanostructures / Metal-metal interactions / N ligands / Nickel / Silver / Palladium

The macrocyclic complexes $[(\eta^5\text{-}C_5H_4C_2\text{-}4\text{-}py)_2Fe]_2Ni_2(NO_3)_4$ (**2**), $[(\eta^5\text{-}C_5H_4C_2\text{-}3\text{-}py)_2Fe]_2Ag_2(ClO_4)_2$ (**4**), and $[(\eta^5\text{-}C_5H_4C_2\text{-}3\text{-}py)_2Fe]_2Pd_2Cl_4$ (**5**) were obtained by reaction of $[Ni(H_2O)_6](NO_3)_2$, $AgClO_4$, and $PdCl_2(COD)$ with the ligands $(\eta^5\text{-}C_5H_4C_2\text{-}4\text{-}py)_2Fe$ (**1**) and $(\eta^5\text{-}C_5H_4C_2\text{-}3\text{-}py)_2Fe$ (**3**), respectively, under high dilution conditions (Scheme 1). The molecular motifs of **2**, **4**, and **5** were studied by single-crystal X-ray structural investigations. Elemental analyses and ^1H NMR and IR spectra were also used to confirm the structures. Compound **2** represents an unsymmetric paddlewheel, in which the centers of the four Cp rings define a nearly ideal rectangle with dimensions of 20.2 × 3.3 Å. In principle, macrocycles **4** and **5** can also be described as rectangles, however, due to the 3-positioned nitrogen donors with deformed edges (17.4 × 3.3 Å for **4**). In contrast to the offset packing of the molecules in **2**, the macrocycles in the crystal of **4** are aligned, with trapped acetonitrile molecules in between. The intra- and intermolecular Ag–Ag distances are 3.50 and 3.79 Å, respectively. Cyclovoltammetric studies reveal chemically reversible ferrocene-based redox reactions of **1**–**4**. Although no electronic communication was observed between the two identical ferrocene units, a weak through-bond electronic interaction between ferrocene and nickel, or silver, was established. In **2** a weak antiferromagnetic interaction between the nickel atoms was also found.

Introduction

A great number of bis(pyridine)-functionalized ligands with different angles between their binding sites have been rationally designed, synthesized, and treated with transition metal complexes to obtain two-dimensional macrocyclic molecular assemblies, such as molecular squares, triangles, and other polygons.[1,2] With the increasing multitude of motifs self-assembled from these nitrogen-functionalized building blocks, a library of such supramolecular architectures has been set up.[3] Stang and Fujita have made a huge contribution to this field, although they have mainly employed pre-constructed *cis*-ML_2 (M = Pd/Pt) units.[1–4] Both metals are electrochemically and magnetically inert. Hence, it is desirable to make accessible molecular polygons and polyhedra with magnetic and redox-active centers.[1,5] Although 1,1′-bis(diphenylphosphanyl)ferrocene (dppf) has been used to obtain redox-active molecular squares, the *syn*-dppf conformer is not part of the backbone.[1,6] A structurally characterized molecular square containing an *anti*-1,1′-ferrocenedicarboxylate moiety in its backbone was recently reported by Cotton et al.[4,5] Compared to systems assembled from non-ferrocene bridges, its electrochemical properties are rather unusual. The preparation of self-assembled structures that contain functionalized sites capable of showing interesting electronic, magnetic, and optical properties is still a big challenge.[1]

Linked metallocenes, in particular those with extended conjugated spacers, are redox-active and good candidates for the investigation of through-bond electronic communication.[7] Ideal models consist of two or more identical metallocene units as spectators.[7,8] It has been demonstrated that acetylene-bridged ferrocenes show third-order non-linear optical properties.[9] Furthermore, systems incorporating paramagnetic transition metal ions are good candidates for novel molecular-based magnetic materials.[10,11] Dinuclear molecules based on dinickel, dicopper, and dimanganese cores, with different magnetic coupling patterns, have drawn much attention in the last decade.[12–14] Here, we present the synthesis and structure of three redox-active tetranuclear supramolecular rectangles **2**, **4**, and **5**, each bearing two ferrocene subunits and two nickel(II), silver(I), and palladium(II) atoms, respectively, in their backbone.

[‡] Preparation, Properties, and Reactions of Metal-Containing Heterocycles, 109. Part 108: Ref.[17]

[a] Institut für Anorganische Chemie der Unversität Tübingen, Auf der Morgenstelle 18, 72076 Tübingen, Germany
Fax: (internat.) + 49-(0)7071/295306
E-mail: ekkehard.lindner@uni-tuebingen.de

Results and Discussion

Syntheses of the Macrocycles 2, 4, and 5

The macrocyclic motifs **2**, **4**, and **5** were obtained in 92−95% yields by mixing a solution of the nitrogen donor ligands 1,1′-bis(4- and 3-pyridylethynyl)ferrocene **1**[15] and **3**[15] in dichloromethane with a solution of $[Ni(OH_2)_6](NO_3)_2$, $AgClO_4$, or $PdCl_2(COD)$ in methanol, acetonitrile, or dichloromethane, respectively, under high-dilution conditions[16] at room temperature (Scheme 1). Elemental analyses are satisfactory and consistent with their proposed structures. While the red silver compound **4** is at least slightly soluble in polar organic media like acetonitrile, the red nickel complex **2** shows only a very low solubility in methanol and acetonitrile. Macrocycle **5** is insoluble in these solvents, but slightly soluble in dichloromethane and DMF. Complex **2** decomposes in DMF and DMSO.

Crystal Structures of 2, 4, and 5

To obtain detailed information about the structures of the nickel(II)-, silver(I)-, and palladium(II)-containing macrocyclic complexes **2**, **4**, and **5**, X-ray structural investigations were performed. Selected distances and angles are summarized in Tables 1 and 2, respectively, and the corresponding ORTEP plots with atom labeling are depicted in Figures 1 and 2. Both compounds **2** and **4** crystallize in the triclinic space group $P\bar{1}$ and each molecule has a center of symmetry. They crystallize with three CH_2Cl_2 and two CH_3CN solvent molecules, respectively.

Table 1. Selected distances [Å] and angles [°] for **2**·3CH_2Cl_2

Ni1−O1	2.081(2)	Ni1−Ni1A	3.39
Ni1−O1A	2.112(2)	Cp1 (cent.)−Cp2 (cent.)	3.31
Ni1−O4	2.120(2)	Fe1−Fe1A	20.18
Ni1−O5	2.079(2)	Cp1 (cent.)−Cp2A (cent.)	20.24
Ni1−N1	2.058(2)	Fe1−Ni1	10.20
Ni1−N2A	2.058(2)	Fe1−Ni1A	10.25
O2−H41A	2.49	O6−H41B	2.42
O3−H40B	2.55		
N1−Ni1−O1	91.58(9)	N2A−Ni1−O5	89.97(9)
N1−Ni1−O1A	92.42(9)	O1−Ni1−O4	115.06(9)
N1−Ni1−O4	89.37(9)	O1−Ni1−O1A	72.22(9)
N1−Ni1−O5	88.28(9)	O5−Ni1−O4	61.40(10)
N2A−Ni1−O1	90.00(9)	O5−Ni1−O1A	111.33(9)
N2A−Ni1−O1A	90.70(9)	N1−Ni1−N2A	176.81(9)
N2A−Ni1−O4	87.45(9)	Ni1−O1−Ni1A	107.79(9)

Both nickel atoms in **2** are octahedrally coordinated by two nitrogen and four oxygen donor functions, forming a *trans*-N_2O_4 coordination sphere. The two *trans*-located nitrogen atoms are equidistant from the nickel atom (2.05 Å), while the four Ni−O bonds have lengths of between 2.08

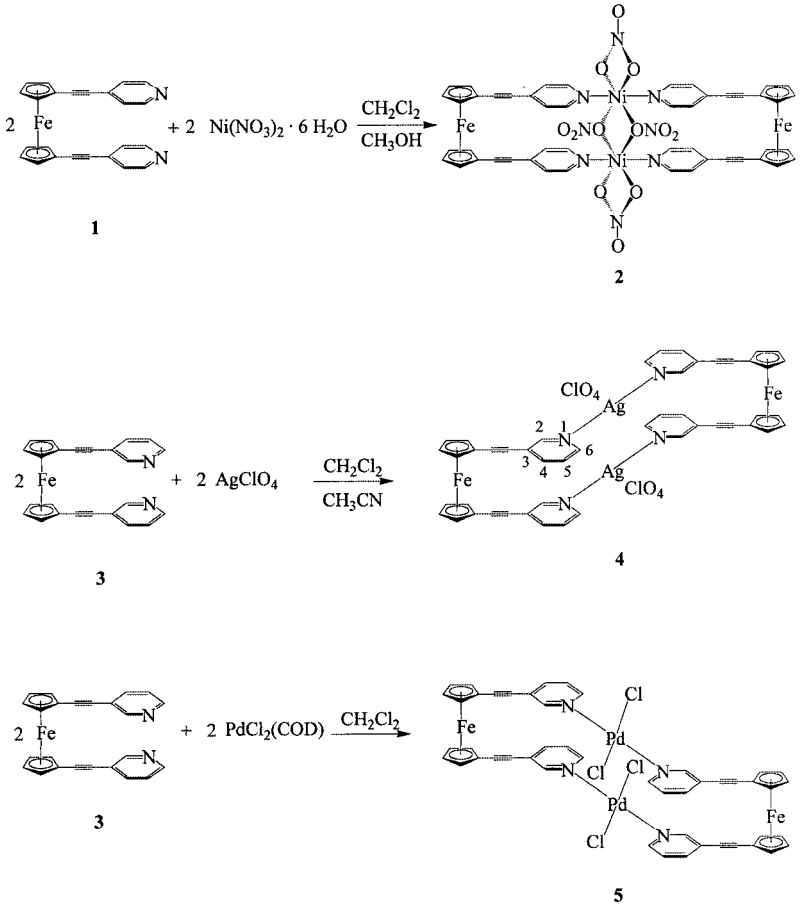

Scheme 1

Table 2. Selected distances [Å] and angles [°] for **4**·2 CH_3CN

Ag1−O1	2.791(2)	Ag1−Ag1A	3.50
Ag1−O1A	3.743(2)	Cp1 (cent.)−Cp2 (cent.)	3.31
Ag1−N1	2.179(2)	Fe1−Fe1A	17.34
Ag1−N2A	2.170(2)	Cp1 (cent.)−Cp2A (cent.)	17.42
Ag1−N3B	2.891(2)	Fe1−Ag1	8.65
Ag1−N3A	2.705(2)	Fe1−Ag1A	9.03
O1−Cl	1.433(2)	Ag1−Ag1 (intermolecular)	3.79
O2−Cl	1.434(2)	O3−Cl	1.434(2)
O4−Cl	1.435(2)		
Cp−py (dihedral)	6.12(4)	py−py (dihedral)	6.17(4)
	13.10(3)	N1−Ag1−N2A	178.1(1)

and 2.12 Å. However, the nickel-centered angles of the octahedron vary between 61 and 115°, indicating a considerably distorted geometry around the nickel atom.

Complex **2** is constructed of a dinickel core with two bridging ligands **1** [μ-η^1:η^1-**1**-*N*,*N*′] and four nitrate counterions. The nitrate ions are coordinated in two different modes to the nickel centers. Two of them function as μ_2-bridging ligands, whereas the other two are η^2-chelated. Within a ligand **1** in complex **2**, the N−N distance of 3.49 Å is significantly shorter than the corresponding average distance of 3.96 Å in the free ligand **1**,[17] in which the repulsion of the nitrogen lone pairs has to be considered.

Concerning the dinickel core, the structure of **2** can be designated as an unsymmetric paddlewheel consisting of the coordinated nitrate ions and two moieties of ligand **1**. The

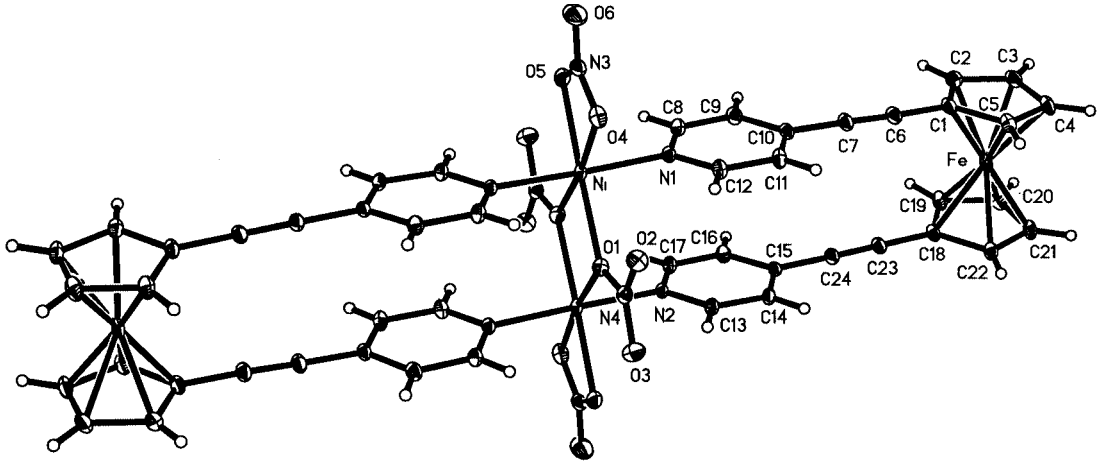

Figure 1. Molecular structure of **2**; ORTEP plot with thermal ellipsoids at 20% probability; solvent molecules are omitted for clarity; for bond lengths and angles see Table 1

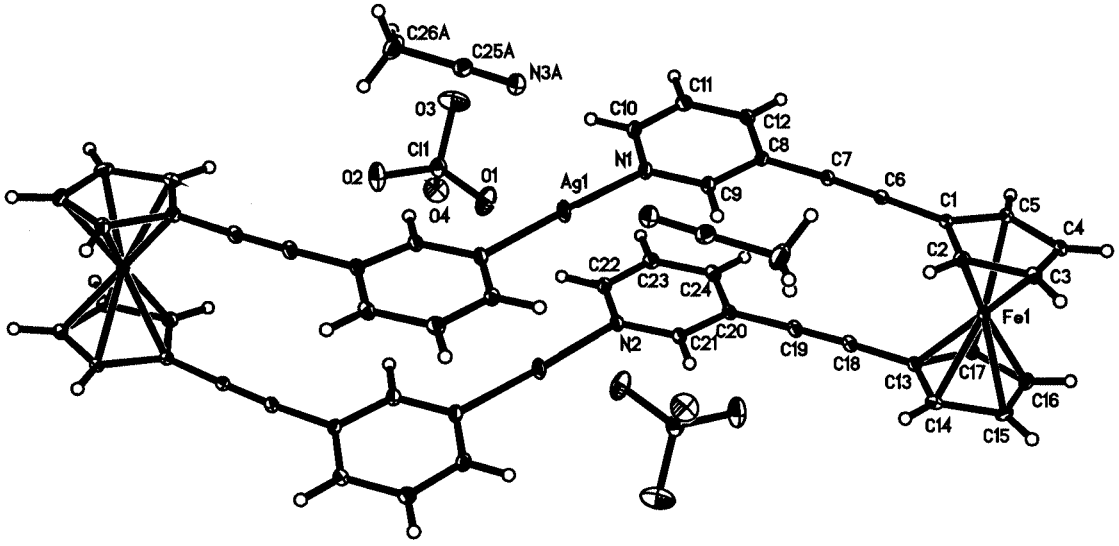

Figure 2. Molecular structure of **4**; ORTEP plot with thermal ellipsoids at 20% probability; for bond lengths and angles see Table 2

whole structure has the shape of a molecular rectangle in which the four Cp rings occupy the vertices, whereas the four metal atoms are located in the middle of the edges. The lengths of the edges are 3.31 and 20.24 Å, calculated from the center points of the cyclopentadienyl rings. Both nickel and iron atoms are separated by a distance of 3.39 and 20.18 Å, respectively. In this molecule the four metal atoms lie in a plane, creating almost a regular rhombus with lengths of 10.20 (Fe−Ni) and 10.25 Å (Fe−NiA) and angles of 19° (Ni−Fe−NiA) and 161° (Fe−Ni−FeA). One of the most important structural features of **2** is the coplanarity of the entire inorganic entity (nickel atoms and all four nitrates). The ferrocene units are positioned above and below this plane. In the solid state, molecules of **2** are offset positioned and separated by two crystallographically different kinds of dichloromethane molecules (Figure 3). Dichloromethane molecules of each kind are oriented head-to-head. Weak contacts (shown by dotted lines in Figure 3) between the solvent molecules and the macrocycles are found, as indicated by the non-bonding distances of 2.42, 2.49, and 2.55 Å for H(41B)−O(2), H(41A)−O(6), and H(40B)−O(3), respectively.

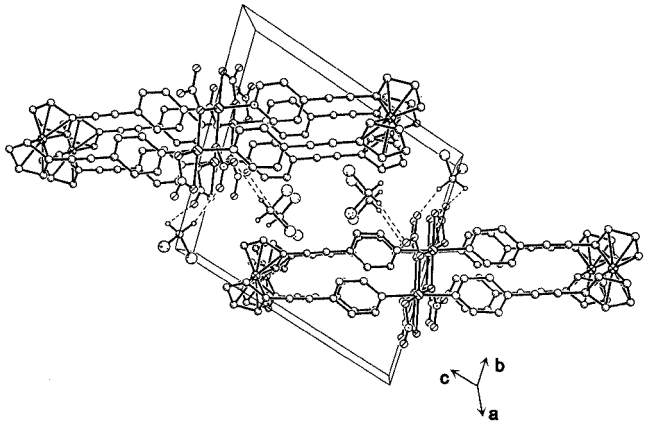

Figure 3. Molecular packing of **2** showing the head-to-head orientation of dichloromethane molecules, the offset arrangement of **2**, and the weak H···O contacts (dotted lines); aromatic protons are omitted for clarity

Due to the 3-position of the nitrogen donors in ligand **3**, the structure of the cation in **4** is somewhat different from that of **2**. The former forms a distorted rectangle defined by the central points of the four cyclopentadienyl rings (Figure 2). If a connecting line is drawn between these points, one pyridine ring is located in front of and the other one behind this line. The dimensions of the rectangle are 17.42 × 3.31 Å. All four transition metals (two silver and two iron atoms) lie in a plane and the Fe−Fe and Ag−Ag distances are 17.34 and 3.50 Å, respectively. The heteroatom distances (Ag−Fe) are 8.65 and 9.03 Å. Similar to complex **2**, the silver atom in **4** is nearly equidistant from the two coordinated pyridine N atoms [2.170(2) and 2.179(2) Å]. Only a slight deviation from a linear N−Ag−N arrangement is observed (178.1°). The two CpC_2py arms on each side of the macrocycle are not oriented exactly parallel, deviations with respect to Cp/py and py/py are 6.1/13.1 and 6.2°, respectively.

In the crystals of **4** (Figure 4), both perchlorate anions are positioned on opposite sides of the rectangular plane, but are not coordinated to silver(I). The macrocycles of **4** are layered and acetonitrile is located between these rectangular molecules. The molecules of **4** are held together along the *a* axis by interactions between the bifurcated acetonitrile molecules and the macrocycles as indicated by the remarkably short Ag−N distances of 2.705(2) and 2.891(2) Å compared to the corresponding sum of the van der Waals radii. The inter- (Ag_2N_2) and intramolecular (Ag_2O_2) planes deviate by an angle of 17.5°. Contrary to the offset packing of macrocycle **2**, the cationic macrocycle **4** is aligned along the *a* axis with intra- and intermolecular Ag−Ag distances of 3.50 and 3.79 Å, respectively.

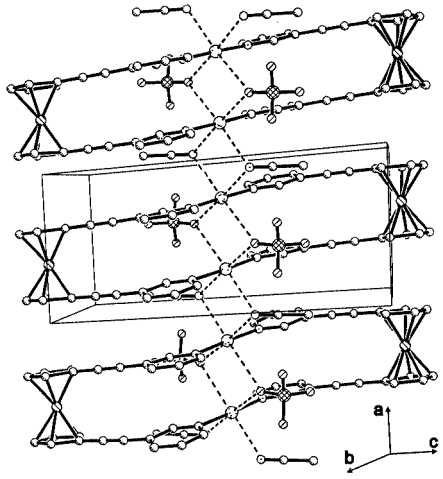

Figure 4. Molecular packing of **4** along the *a* axis presenting the parallel alignment of the silver ions and the other components as well as the weak Ag···O and Ag···N contacts (dotted lines); protons are omitted for clarity

Due to the low quality of the crystal of **5**, only a brief description is given.[18,19] The molecular structure of **5** is similar to that of **4**, and also has a center of symmetry. Each palladium atom is additionally coordinated by two *trans*-positioned chloride ions with $PdCl_2$ units about 45° to the pyridine rings.

^{1}H NMR and IR Spectroscopic Characterization of the Macrocycles 2, 4, and 5

Because of the low solubility only ^{1}H NMR spectra of the macrocycles **4** and **5** could be recorded; the nickel(II) complex **2** is paramagnetic. Upon complexation of ligand **3** to silver(I) (**4**) and palladium(II) (**5**) a slight downfield shift of the pyridine proton signals is observed. While only the resonance at δ = 7.05 ppm, which is assigned to 5-H of the pyridine ring in **3** (numbering scheme is given in Scheme 1), is markedly downfield shifted to δ = 7.20 ppm in the disilver complex **4**, all other protons of this entity remain unchanged. In the ^{1}H NMR spectrum of **5** the protons (2-H and 6-H) adjacent to the nitrogen atom give rise to a re-

markable downfield shift of 0.18 and 0.31 ppm, respectively. On the other hand, notable upfield shifts of 0.27 and 0.31 ppm are observed for 4-H and 5-H. The AA′XX′ pattern for the cyclopentadienyl rings in the spectra of **4** and **5** remains unchanged.

In the FT-IR spectra of **2**, **4**, and **5** the absorptions for the C=N and C≡C stretching vibrations are shifted (12−16 and 2−5 cm^{-1}, respectively) to somewhat higher wavenumbers relative to the free ligands **1** and **3**. This is consistent with the coordination of transition metals to nitrogen. Intense bands at 1289/1218 and 1095/1050 cm^{-1} are assigned to the stretching vibrations of the nitrate and perchlorate anions, respectively.

Electrochemical Investigation of 1−4

The redox properties of compounds **1**−**4** were investigated in acetonitrile; cyclic voltammetric data are listed in Table 3. The low solubility of the palladium complex **5** prevents any studies of its electrochemical behavior. Although the ferrocene-based redox reactions of **1**−**4** are chemically reversible in each case, their electrochemistry is somewhat different. While ligand **3** shows a diffusion-controlled one-electron transfer reaction, the response of ligand **1** is diffusion-controlled and dependent on the rate of electron transfer. Isomeric ligands **1** and **3** show different redox potentials, at 318 and 283 mV relative to that of ferrocene/ferrocenium, respectively. They are more difficult to oxidize than the unsubstituted parent ferrocene, which is due to the electron-withdrawing nature of the substituents on the Cp rings. However, the difference of 35 mV between **1** and **3** indicates the influence of the charge distribution on the transfer of this effect. Although both ferrocene subunits of complex **2** are oxidized at the same potential, it reveals a 32 mV positive shift relative to ligand **1**. This finding demonstrates a successful electron transfer from ferrocene to the nickel atoms, but no communication between the two ferrocene units.

Table 3. Cyclic voltammetric responses of compounds **1**−**4** in acetonitrile

Compound	$E_{1/2}$ [mV]	ΔE [mV]	i_{pa}/i_{pc}
Ferrocene	0	69	1.00
1	318	63	0.99
2	350	60	1.16[a]
3	283	71	0.96
4	273	70	1.04

[a] A background correction was not carried out because of the adsorption nature of this complex.

Compared to ligand **3** a negative shift of 10 mV was established for the disilver complex **4**. This effect is usually not expected and is probably due to the weak σ-electron acceptor and strong π-donor capabilities of silver(I).[20] As a result of this back bonding and/or the charge distribution

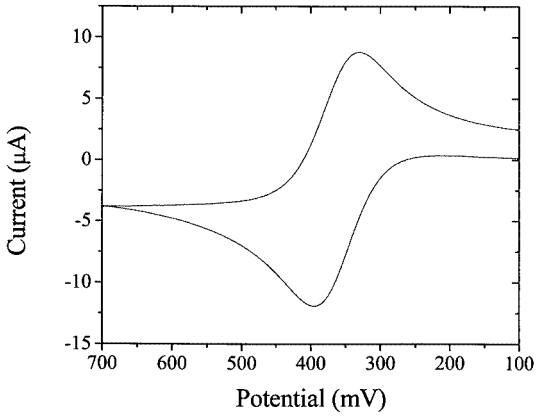

Figure 5. Cyclic voltammogram of **4** in acetonitrile/0.1 M tetrabutylammonium hexafluorophosphate; concentration of **4**: $1 \cdot 10^{-4}$ M, scan rate of 100 mV/s

order the ferrocene moieties are easily oxidized. Figure 5 shows the cyclic voltammogram of complex **4**, the electrochemical response of which is diffusion-controlled, whereas that of the dinickel complex **2** is more complicated due to its adsorption character.

For a possible electronic communication between the two ferrocene units the intramolecular iron−iron distances (**2**: 2.0 nm; **4**: 1.7 nm) are of importance. Because of the well-separated ferrocene building blocks the coulombic interaction (through-space electronic coupling) is negligible. On the other hand, the alignment of the molecular orbitals[21] and the extent of conjugation[7] could be a reason for through-bond electronic communication, as was observed in a conjugated alkyne-bridged rhenium(II) complex.[22] In spite of these favorable preconditions no electronic communication was found in complexes **2** and **4**.

Magnetic Investigation of Complex 2

The magnetic properties of the dinickel complex **2** were studied at 10 T in the temperature range between 300 and 5 K. Experimental data obtained for the molar susceptibility and the calculated effective magnetic moment are plotted in Figure 6. The general isotropic spin-Hamiltonian expression for the symmetrical dinickel compound is $\mathbf{H} = -J\mathbf{S_A}\cdot\mathbf{S_B}$ ($S_A = S_B = 1$), where J is the coupling constant between the two nickel(II) atoms. Although no maximum for χ_M in Figure 6 is found in the selected temperature range, a non-linear fit of the experimental data for the susceptibility per nickel dimer using published expressions[23] yields the following values: $g = 2.22 \pm 0.01$, $J = -17.37 \pm 0.24$ cm^{-1}, $D = 7.87 \pm 0.17$ cm^{-1}, and $p = 17.6 \pm 0.1\%$. The g value is reasonable for octahedrally coordinated nickel(II),[13] and the coupling constant reveals a weak, intramolecular, antiferromagnetic interaction between the nickel(II) atoms. This coupling for the bis(μ-oxo)-bridged dinickel(II) complex **2** (Ni−Ni distance of 3.39 Å) is more significant than that observed for other dinickel complexes in which two bridges consisting of two or more atoms are present and both nickel units are separated by distances of between 4.16 and 4.32 Å,[13] although it is cle-

arly weaker than that of cyano-bridged dinickel complexes.[12] Complex **2** also contains an uncoupled paramagnetic impurity which is a chain-like polymer or oligomer[24] which is formed even under high-dilution conditions. This could not be separated from **2** because both entities show very low solubility. The agreement factor $R = 9.8 \cdot 10^{-5}$ shows that the curve is well fitted.

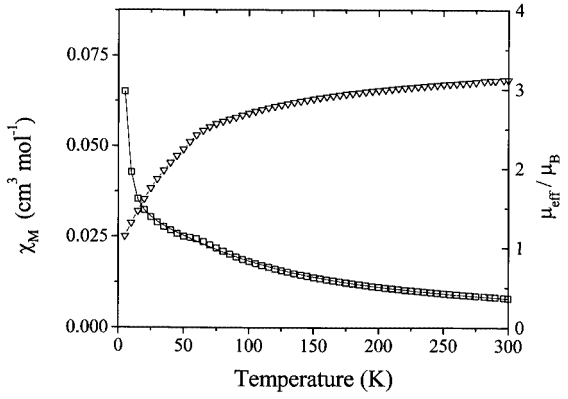

Figure 6. Temperature dependence of the magnetic susceptibility (squares, left scale) and effective magnetic moment (triangles, right scale) of **2**; the solid lines represent the best-fit curves

Conclusion

Functionalized heterotetranuclear regular and distorted rectangles bearing two redox-active ferrocene subunits and a pair of transition metal atoms each were made accessible by coordination-driven spontaneous self-assembly. Although silver is considerably bigger than nickel the separation between the two equal transition metal atoms in the dimetallic Ag_2 and Ni_2 cores is rather similar (3.50 vs. 3.39 Å). This behavior is mainly controlled by the kind of ligands employed (**1** or **3**). Due to the different positions of the nitrogen atoms in ligands **1** and **3**, the molecular structure of **2** is an ideal rectangle, whereas **4** and **5** are deformed rectangles. No long-range through-bond electronic communication was established in the macrocyclic complexes **2** and **4**. Two factors should mainly be responsible for this observation: (i) both ferrocene building blocks are separated by a distance of more than 1.7 nm, and are thus too far away to communicate, and (ii) the Ni_2 and Ag_2 cores fail to transmit the Cp−C≡C−py conjugation.[25] However, a weak influence of the Ni^{II} and Ag^{I} atoms on the redox potential of the ferrocene units has been established through the conjugated bonds in spite of a separation of 1 nm. In the case of the nickel(II) complex **2**, a weak antiferromagnetic interaction between the intramolecularly arranged nickel(II) atoms was found.

Experimental Section

General Remarks: All reactions and manipulations were carried out under argon by use of standard Schlenk techniques except otherwise noted. Acetonitrile and dichloromethane were dried with calcium hydride and distilled, degassed, and stored under argon. FT-IR data were obtained with a Bruker IFS 48 FT-IR spectrometer. The EI mass spectrum of ligand **3** was recorded with a Finnigan TSQ 70 (200°C) instrument. ^1H and $^{13}C\{^1H\}$ NMR spectra were recorded at 25 °C with a Bruker DRX 250 spectrometer operating at 250.13 and 62.90 MHz, respectively. ^1H and ^{13}C NMR chemical shifts are referenced to partially deuterated and deuterated solvent peaks, and are reported relative to TMS. Elemental analyses were carried out with an Elementar Vario EL analyzer. All electrochemical experiments were performed with a Bioanalytical CV-50W Voltammetric Analyzer (BAS, West Lafayette, IN, USA) controlled by a standard 80486 personal computer (control program version 2.0). For electroanalytical experiments a Metrohm platinum-tip electrode (Filderstadt, Germany) was applied as working electrode. The counter electrode was a platinum wire of 1 mm in diameter. A single-unit Haber-Luggin Ag^+/Ag double reference electrode was used. The resulting potential values are referenced to Ag/Ag^+ (0.01 M in CH_3CN/0.1 M Bu_4NPF_6). Ferrocene was used as an external standard. Its potential of 102.5 mV was determined by separate cyclic voltammetric experiments in the respective solvent, and all potentials in the present paper are reported relative to the fc/fc^+ standard. For cyclic voltammetry, a glass-tight full-glass three-electrode cell was used; its assembly for the experiments has been described previously.[26] The cell was purged with argon before it was filled with the electrolyte. Background curves were recorded before adding the substrate to the solution. These were later subtracted from the experimental data of the samples (excluding complex **2**). The automatic BAS CV-50 W *iR*-drop compensation facility was used for all experiments. Magnetic susceptibility of a powdered sample packed in a capsule was measured using a SQUID Quantum Design MPMS magnetometer at 10000 Gauss over the temperature range 5−300 K. All data were corrected for sample-holder contribution. The diamagnetism of the sample and paramagnetism of nickel(II) were represented by a parameter in the non-linear fit equation. This parameter was found to be $(5.4 \pm 1.4) \times 10^{-4}$ emu/mol. Compounds **1**,[15] **3**,[15] and $[PdCl_2(COD)]$[27] were synthesized according to literature methods. $AgClO_4$ and $Ni(NO_3)_2 \cdot 6H_2O$, were used as received without further treatment.

Complex 2: Solutions of nickel(II) nitrate hexahydrate (74 mg, 0.25 mmol) in methanol (50 mL) and of ligand **1**[15] (98 mg, 0.25 mmol) in dichloromethane (50 mL) were simultaneously added dropwise to a stirred mixture of dichloromethane and methanol (50/50 mL) within 4 h at room temperature. The resulting red mixture was stirred for 20 h at the same temperature. Then, the solvents were removed under vacuum. The red residue was washed with methanol (2 mL) and dichloromethane (5 mL) and dried in vacuo for 15 h. Yield 136 mg (92%), red solid, m.p. > 270°C. FT-IR (KBr, cm^{-1}): $\tilde{\nu}$ = 2207 s (C≡C), 1611 vs (C=N), 1289 s (NO_3^-), 1218 sh (NO_3^-). $C_{48}H_{32}Fe_2N_8Ni_2O_{12} \cdot 0.5CH_2Cl_2$ (1184.37): calcd. C 49.18, H 2.81, N 9.46; found C 49.12 H, 2.88 N 9.25.

Ligand 3: This ligand was prepared by a published method,[15] and further purified by recrystallization from dichloromethane and acetonitrile. Red crystals, m.p. 195°C. ^1H NMR (CD_2Cl_2, ppm): δ = 8.50 (dd, $^4J_{H,H}$ = 2.20, $^5J_{H,H}$ = 0.82 Hz, 4 H, 2-H, C_5H_4N), 8.35 (dd, $^3J_{H,H}$ = 4.87, $^4J_{H,H}$ = 1.73 Hz, 4 H, 6-H, C_5H_4N), 7.63 (ddd, $^3J_{H,H}$ = 7.91, $^4J_{H,H}$ = 1.92, $^4J_{H,H}$ = 1.92 Hz, 4 H, 4-H, C_5H_4N), 7.05 (ddd, $^3J_{H,H}$ = 7.91, $^4J_{H,H}$ = 4.87, $^5J_{H,H}$ = 0.82 Hz, 4 H, 5-H, C_5H_4N), 4.50 (m,[28] 8 H, C_4H_4C), 4.29 (m,[29] 8 H, C_4H_4C). $^{13}C\{^1H\}$ NMR (CD_2Cl_2, ppm): δ = 152.17 (C-2), 148.23 (C-6), 138.11 (C-4), 123.24 (C-5), 121.10 (C-3), 90.55, 83.79 (C≡C), 73.38,

71.41 (C_4H_4C), 66.96 (C_4H_4C). MS (EI); *m/z*: 388.0 [M^+]. IR (KBr, cm^{-1}): $\tilde{\nu}$ = 2206 s (C≡C), 1581 w (C=N). $C_{24}H_{16}FeN_2 \cdot 0.05CH_2Cl_2$ (392.50): calcd. C 73.60, H 4.13, N 7.14; found C 73.44, H 4.18, N 6.98.

Complex 4: Solutions of ligand **3** (42 mg, 0.108 mmol) in a mixture of acetonitrile/dichloromethane (25/2 mL) and of silver(I) perchlorate (23.5 mg, 0.114 mmol) in acetonitrile (20 mL) were simultaneously added dropwise to stirred dichloromethane (20 mL) at room temperature during a period of 2 h. After the addition, the mixture was stirred for 24 h at the same temperature followed by the removal of solvents under vacuum. The precipitate was filtered (P3) and washed with dichloromethane (3 mL) and finally dried in vacuo. ***WARNING:*** *This perchlorate complex is hazardous because of the possibility of explosion! Compound* ***4*** *exploded at about 220 °C during the measurement of the melting point! Special care should therefore be taken and only very small amounts of the sample should be handled!* Yield 64.5 mg (94%), red powder, m.p. > 220°C (*explosive!*). ^{1}H NMR (CD_3CN, ppm): δ = 8.49 (dd, $^4J_{H,H}$ = 2.20, $^5J_{H,H}$ = 0.71 Hz, 4 H, 2-H, C_5H_4N), 8.41 (dd, $^3J_{H,H}$ = 4.94, $^4J_{H,H}$ = 1.57 Hz, 4 H, 6-H, C_5H_4N), 7.64 (ddd, $^3J_{H,H}$ = 7.98, $^4J_{H,H}$ = 1.88, $^4J_{H,H}$ = 1.88 Hz, 4 H, 4-H, C_5H_4N), 7.20 (ddd, $^3J_{H,H}$ = 7.98, $^4J_{H,H}$ = 4.94, $^5J_{H,H}$ = 0.71 Hz, 4 H, 5-H, C_5H_4N), 4.50 (m,[28] 8 H, C_4H_4C), 4.29 (m,[29] 8 H, C_4H_4C). IR (KBr, cm^{-1}): $\tilde{\nu}$ = 2211 m (C≡C), 1593 w (C=N), 1095 vs, 1050 s (ClO_4^-). $C_{48}H_{32}Ag_2Cl_2Fe_2N_4O_8 \cdot CH_3CN \cdot 0.5\ CH_2Cl_2$ (1274.66): calcd. C 47.59, H 2.85, N 5.49; found C 47.30, H 2.83, N 5.30.

Complex 5: Solutions of ligand **3** (77 mg, 0.2 mmol) in dichloromethane (50 mL) and of [$PdCl_2$(COD)] (57 mg, 0.2 mmol) in dichloromethane (50 mL) were simultaneously added dropwise to stirred dichloromethane (50 mL) at room temperature during a period of 1 h. After the addition, the mixture was stirred for 20 h at the same temperature followed by the removal of solvents under vacuum. The precipitate was filtered and washed with dichloromethane (3 mL) and finally dried in vacuo. Yield 107 mg (95%), red powder, m.p. > 270 °C. ^{1}H NMR (CD_2Cl_2, ppm): δ = 8.68 (d, $^4J_{H,H}$ = 2.51 Hz, 4 H, 2-H, C_5H_4N), 8.66 (dd, $^3J_{H,H}$ = 6.08, $^4J_{H,H}$ = 1.30 Hz, 4 H, 6-H, C_5H_4N), 7.36 (ddd, $^3J_{H,H}$ = 7.96, $^4J_{H,H}$ = 1.90, $^4J_{H,H}$ = 1.90 Hz, 4 H, 4-H, C_5H_4N), 6.74 (ddd, $^3J_{H,H}$ = 7.96, $^4J_{H,H}$ = 6.08, $^5J_{H,H}$ = 0.67 Hz, 4 H, 5-H, C_5H_4N), 4.55 (m,[28] 8 H, C_4H_4C), 4.30 (m,[29] 8 H, C_4H_4C). IR (KBr, cm^{-1}): $\tilde{\nu}$ = 2209 s (C≡C), 1596 w (C=N), 1095 vs, 1050 s (ClO_4^-). $C_{48}H_{32}Cl_4Fe_2N_4Pd_2$ (1131.15): calcd. C 50.97, H 2.85, Cl 12.54, N 4.95; found C 50.58, H 2.68, Cl 12.57, N 4.83.

X-ray Crystallographic Study: Crystallographic and data collection information as well as a description of the structural analyses and refinements for complexes **2** and **4** are summarized in Table 4. Single crystals of **2** were obtained by slow diffusion of a solution of ligand **1** in dichloromethane into a solution of nickel(II) nitrate hexahydrate in methanol.[30] Suitable single crystals of **4** were obtained by slow diffusion of a solution of ligand **3** in dichloromethane into a solution of silver(I) perchlorate in acetonitrile. Crystals of **5** were obtained by slow diffusion of a [$PdCl_2$(COD)] solution

Table 4. Crystal data and structure refinement for **2** and **4**

	2·3CH_2Cl_2	**4**·2CH_3CN
Empirical formula	$C_{51}H_{38}Cl_6Fe_2N_8Ni_2O_{12}$	$C_{52}H_{38}Ag_2Cl_2Fe_2N_6O_8$
Formula mass	1396.72	1273.22
Crystal system	triclinic	triclinic
Space group	$P\bar{1}$	$P\bar{1}$
a [Å]	8.0907(17)	7.0579(8)
b [Å]	13.424(2)	10.5149(10)
c [Å]	13.955(2)	16.5415(15)
α [°]	71.455(9)	75.829(7)
β [°]	75.946(11)	85.663(9)
γ [°]	75.045(14)	85.196(8)
V [Å^3]	1366.7(4)	1184.1(2)
Z	1	1
$d_{calcd.}$ [g·cm^{-3}]	1.697	1.785
Temperature [K]	173(2)	173(2)
F(000)	706	636
Crystal size [mm]	0.1×0.4×0.4	0.1×0.8×0.2
Wavelength [Å]	0.71073	0.71073
θ limits [°]	2.55 to 27.49	2.00 to 27.50
hkl ranges	$-10 \le h \le 8$	$-9 \le h \le 9$
	$-16 \le k \le 16$	$-13 \le k \le 13$
	$-17 \le l \le 18$	$-21 \le l \le 21$
Reflections collected	11739	10851
Reflections unique	6214 (R_{int} = 0.0255)	5426 (R_{int} = 0.0189)
Completeness to θ = max.	99.0%	99.7%
Absorption correction	empirical	empirical
Max. and min. transmission	0.3614 and 0.2643	0.5151 and 0.3983
Refinement method	full-matrix least-squares on F^2	full-matrix least-squares on F^2
Data/restraints/parameters	6214/0/380	5426/0/327
Goodness of fit on F^2	1.021	1.072
Final *R* indices [$I > 2\sigma(I)$][a]	$R1$ = 0.0425, wR_2 = 0.1115	$R1$ = 0.0236, wR_2 = 0.0613
R indices (all data)	$R1$ = 0.0561, wR_2 = 0.1189	$R1$ = 0.0272, wR_2 = 0.0630
Extinction coefficient	0.0024	0.0082(4)
Largest diff. peak and hole [e·Å^{-3}]	1.175 and −0.696	0.520 and −0.500

[a] $R_1 = ||F_o| - |F_c||/|F_o|$; $wR_2 = \{[w(F_o^2 - F_c^2)^2]/[w(F_o^2)^2]\}^{0.5}$.

in dichloromethane into a dichloromethane solution of ligand **3** at room temperature. Each crystal was fixed on a glass fiber using perfluoropolyether RS 3000 and transferred to a Siemens P4 diffractometer (**2**, **4**) or a Stoe IPDS diffractometer (**5**) equipped with a graphite-monochromated Mo-K_α radiation unit. The lattice constants for both macrocycles **2** and **4** were determined by 50 precisely centered high-angle reflections. Intensities were collected by the ω-scan technique. An empirical absorption correction was performed in each case. The structures of **2** and **4** were solved by direct methods with SHELXTL V5.1 (NT version)[31] and refined by least-squares methods with the same program, with anisotropic thermal parameters for all non-hydrogen atoms. All hydrogen atoms were located in calculated positions (riding mode). In **2**, one of the dichloromethane molecules (near the corner of the unit cell in Figure 3) is disordered about the center of inversion. The largest peak and hole in the last difference synthesis were 1.175/−0.696 (**2**), and 0.520/−0.500 (**4**) e·Å^{-3}, respectively. The structure of **5** was solved by direct methods with SHELXS.[32] CCDC-190120 (**2**) and -190121 (**4**) contain the supplementary crystallographic data for this paper. These data can be obtained free of charge at www.ccdc.cam.ac.uk/conts/retrieving.html [or from the Cambridge Crystallographic Data Center, 12 Union Road, Cambridge CB2 1EZ, UK; Fax: (internat.) + 44-1223/336-033; E-mail: deposit@ccdc.cam.ac.uk].

Acknowledgments

Support of this research by the Deutsche Forschungsgemeinschaft and the Fonds der Chemischen Industrie is gratefully acknowledged. Degussa AG is thanked for supplying starting materials. We thank Prof. B. Speiser and Prof. H.-J. Meyer for their helpful discussions and suggestions.

[1] S. Leininger, B. Olenyuk, P. J. Stang, *Chem. Rev.* **2000**, *100*, 853−908.
[2] M. Fujita, *Chem. Soc. Rev.* **1998**, *27*, 417−425.
[3] B. Olenyuk, A. Fechtenkötter, P. J. Stang, *J. Chem. Soc., Dalton Trans.* **1998**, 1707−1728.
[4] F. A. Cotton, C. Lin, C. A. Murillo, *Inorg. Chem.* **2001**, *40*, 478−484.
[5] F. A. Cotton, L. M. Daniels, C. Lin, C. A. Murillo, *J. Am. Chem. Soc.* **1999**, *121*, 4538−4539.
[6] P. J. Stang, B. Olenyuk, J. Fan, A. M. Arif, *Organometallics* **1996**, *15*, 904−908.
[7] S. Barlow, D. O'Hare, *Chem. Rev.* **1997**, *97*, 637−669.
[8] F. Barriere, N. Camire, W. E. Geiger, U. T. Mueller-Westerhoff, R. Sanders, *J. Am. Chem. Soc.* **2002**, *124*, 7262−7263.
[9] Z. Yuan, G. Stringer, I. R. Jobe, D. Kreller, K. Scott, L. Koch, N. J. Taylor, T. B. Marder, *J. Organomet. Chem.* **1993**, *452*, 115−120.
[10] M. Pilkington, S. Decurtins, *Chimia* **2001**, *55*, 1014−1016.
[11] J. C. Noveron, M. S. Lah, R. E. Del Sesto, A. M. Arif, J. S. Miller, P. J. Stang, *J. Am. Chem. Soc.* **2002**, *124*, 6613−6625.
[12] A. Rodriguez-Fortea, P. Alemany, S. Alvarez, E. Ruiz, A. Scuiller, C. Decroix, V. Marvaud, J. Vaissermann, M. Verdaguer, I. Rosenman, M. Julve, *Inorg. Chem.* **2001**, *40*, 5868−5877.
[13] M. Conrad, F. Meyer, A. Jacobi, P. Kircher, P. Rutsch, L. Zsolnai, *Inorg. Chem.* **1999**, *38*, 4559−4566.
[14] D. Volkmer, A. Hörstmann, K. Griesar, W. Haase, B. Krebs, *Inorg. Chem.* **1996**, *35*, 1132−1135.
[15] E. Lindner, R. F. Zong, K. Eichele, *Phosphorus, Sulfur Silicon* **2001**, *169*, 219−222.
[16] P. Knops, N. Sendhoff, H.-B. Mekelburger, F. Vögtle, *High Dilution Reactions − New Synthetic Applications: Topics in Current Chemistry* (Eds.: E. Weber, F. Vögtle), Springer, Heidelberg, **1992**.
[17] E. Lindner, R. F. Zong, K. Eichele, M. Ströbele, *J. Organomet. Chem.* **2002**, *660*, 78−84.
[18] Complex **5**, monoclinic, space group $P2_1/c$, molecular formula: $C_{48}H_{32}Cl_4Fe_2N_4Pd_2$, formula weight: 1131.08, a = 6.7738(14), b = 13.508(3), c = 24.351(5) Å, β = 96.73(3)°, V = 2212.7(8) Å^3, and Z = 2.
[19] R. F. Zong, Dissertation, University of Tübingen, Germany **2002**.
[20] A. N. Khlobystov, A. J. Blake, N. R. Champness, D. A. Lemenovskii, A. G. Majouga, N. V. Zyk, M. Schröder, *Coord. Chem. Rev.* **2001**, *222*, 155−192.
[21] J. V. Ortega, B. Hong, S. Ghosal, J. C. Hemminger, B. Breedlove, C. P. Kubiak, *Inorg. Chem.* **1999**, *38*, 5102−5112.
[22] M. Brady, W. Q. Weng, J. A. Gladysz, *J. Chem. Soc., Chem. Commun.* **1994**, 2655−2666.
[23] D. Volkmer, A. Hörstmann, K. Griesar, W. Haase, B. Krebs, *Inorg. Chem.* **1996**, *35*, 1132−1135.
[24] W. M. Xue, F. E. Kühn, E. Herdtweck, Q. C. Li, *Eur. J. Inorg. Chem.* **2001**, 213−221.
[25] O. Lavastre, J. Plass, P. Bachmann, S. Guesmi, C. Moinet, P. H. Dixneuf, *Organometallics* **1997**, *16*, 184−189.
[26] S. Dümmling, E. Eichhorn, S. Schneider, B. Speiser, M. Würde, *Curr. Sep.* **1996**, *15*, 53−56.
[27] D. Drew, J. R. Doyle, *Inorg. Synth.* **1990**, *28*, 346−349.
[28] m: low-field part of an AA′XX′ pattern, $N = |^3J_{H,H} + {}^5J_{H,H}|$.
[29] m: high-field part of an AA′XX′ pattern, $N = |^3J_{H,H} + {}^5J_{H,H}|$.
[30] V. Jullien, M. W. Hosseini, J. -M. Planeix, A. D. Cian, *J. Organomet. Chem.* **2002**, *634/644*, 376−380.
[31] G. M. Sheldrick, *SHELXTL V5.03, Program for crystal structure refinement*, University of Göttingen, Germany **1995**.
[32] G. M. Sheldrick, *Acta Crystallogr., Sect. A* **1995**, *51*, 33−38. *SHELXS V5.03 program for crystal structure solution*, University of Göttingen, Germany).

Received July 24, 2002
[I02413]